Visible-pulse generation in gain crystal of near-infrared femtosecond optical parametric oscillator

Tae-Young Jeong,[1] Seung-Hyun Kim,[1,2] Geon-Hee Kim,[2] and Ki-Ju Yee[1,*]

[1]*Department of Physics, Chungnam National University, Daejeon 305-764, South Korea*
[2]*Korea Basic Science Institute (KBSI), Daejeon 305-333, South Korea*
[*]*kyee@cnu.ac.kr*

Abstract: An optical parametric oscillator (OPO) based on magnesium-oxide-doped periodically poled lithium niobate (MgO:PPLN) is demonstrated to deliver visible femtosecond pulses, which were created through the intra-cavity nonlinear interactions within the PPLN itself. The signal from the OPO produces femtosecond pulses in the near-infrared region tunable from 1050 to 1600 nm. Visible femtosecond pulses in the range of 522–800 nm and those of 455–540 nm, respectively, were generated via second-harmonic generation (SHG) of signal photons and through sum-frequency generation (SFG) of pump and signal photons. Maximum output efficiencies of 9.2% at 614 nm and 8.0% at 522 nm for the SHG and SFG are attained, respectively, where the efficient visible pulse generation relies on the quasi-phase matching with the aid of the higher-order grating momentum.

OCIS codes: (190.4970) Parametric oscillators and amplifiers; (190.4410) Nonlinear optics, parametric processes; (140.7090) Ultrafast lasers.

References and links

1. M. Ghotbi, A. Esteban-Martin, and M. Ebrahim-Zadeh, "Tunable, high-repetition-rate, femtosecond pulse generation in the ultraviolet," Opt. Lett. **33**(4), 345–347 (2008).
2. T. J. Driscoll, G. M. Gale, and F. Hache, "Ti:sapphire second-harmonic-pumped visible range femtosecond optical parametric oscillator," Opt. Commun. **110**(5-6), 638–644 (1994).
3. D. C. Edelstein, E. S. Wachman, and C. L. Tang, "Broadly tunable high repetition rate femtosecond optical parametric oscillator," Appl. Phys. Lett. **54**(18), 1728–1730 (1989).
4. Z. Zhang, D. T. Reid, S. Chaitanya Kumar, M. Ebrahim-Zadeh, P. G. Schunemann, K. T. Zawilski, and C. R. Howle, "Femtosecond-laser pumped $CdSiP_2$ optical parametric oscillator producing 100 MHz pulses centered at 6.2 μm," Opt. Lett. **38**(23), 5110–5113 (2013).
5. K. J. Yee, J. H. Kim, M. H. Jung, B. H. Hong, and K. J. Kong, "Ultrafast modulation of optical transitions in monolayer and multilayer graphene," Carbon **49**(14), 4781–4785 (2011).
6. H. Chen, H. Wang, M. N. Slipchenko, Y. Jung, Y. Shi, J. Zhu, K. K. Buhman, and J. X. Cheng, "A multimodal platform for nonlinear optical microscopy and microspectroscopy," Opt. Express **17**(3), 1282–1290 (2009).
7. J. E. Schaar, K. L. Vodopyanov, and M. M. Fejer, "Intracavity terahertz-wave generation in a synchronously pumped optical parametric oscillator using quasi-phase-matched GaAs," Opt. Lett. **32**(10), 1284–1286 (2007).
8. Y. Jin, S. M. Cristescu, F. J. M. Harren, and J. Mandon, "Two-crystal mid-infrared optical parametric oscillator for absorption and dispersion dual-comb spectroscopy," Opt. Lett. **39**(11), 3270–3273 (2014).
9. G. D. Miller, R. G. Batchko, W. M. Tulloch, D. R. Weise, M. M. Fejer, and R. L. Byer, "42%-efficient single-pass cw second-harmonic generation in periodically poled lithium niobate," Opt. Lett. **22**(24), 1834–1836 (1997).
10. K. Fradkin, A. Arie, A. Skliar, and G. Rosenman, "Tunable midinfrared source by difference frequency generation in bulk periodically poled $KTiOPO_4$," Appl. Phys. Lett. **74**(7), 914–916 (1999).
11. R. V. Roussev, C. Langrock, J. R. Kurz, and M. M. Fejer, "Periodically poled lithium niobate waveguide sum-frequency generator for efficient single-photon detection at communication wavelengths," Opt. Lett. **29**(13), 1518–1520 (2004).
12. K. Sasagawa and M. Tsuchiya, "Highly efficient third harmonic generation in a periodically poled $MgO:LiNbO_3$ disk resonator," Appl. Phys. Express **2**(12), 122401 (2009).

#247576 Received 7 Aug 2015; revised 12 Sep 2015; accepted 14 Sep 2015; published 21 Sep 2015

13. A. Esteban-Martin, O. Kokabee, and M. Ebrahim-Zadeh, "Efficient, high-repetition-rate, femtosecond optical parametric oscillator tunable in the red," Opt. Lett. **33**(22), 2650–2652 (2008).
14. F. Ruebel, P. Haag, and J. A. L'huillier, "Synchronously pumped femtosecond optical parametric oscillator with integrated sum frequency generation," Appl. Phys. Lett. **92**(1), 011122 (2008).
15. S. Mieth, A. Henderson, and T. Halfmann, "Tunable, continuous-wave optical parametric oscillator with more than 1W output power in the orange visible spectrum," Opt. Express **22**(9), 11182–11191 (2014).
16. H. Y. Shen, H. Xu, Z. D. Zeng, W. X. Lin, R. F. Wu, and G. F. Xu, "Measurement of refractive indices and thermal refractive-index coefficients of $LiNbO_3$ crystal doped with 5 mol. % MgO," Appl. Opt. **31**(31), 6695–6697 (1992).
17. K. J. Han, D. W. Jang, J. H. Kim, C. K. Min, T. H. Joo, Y. S. Lim, D. Lee, and K. J. Yee, "Synchronously pumped optical parametric oscillator based on periodically poled MgO-doped lithium niobate," Opt. Express **16**(8), 5299–5304 (2008).
18. K. C. Burr, C. L. Tang, M. A. Arbore, and M. M. Fejer, "High-repetition-rate femtosecond optical parametric oscillator based on periodically poled lithium niobate," Opt. Lett. **70**, 3341–3343 (1997).
19. B. Proctor, E. Westwig, and F. Wise, "Characterization of a Kerr-lens mode-locked Ti:sapphire laser with positive group-velocity dispersion," Opt. Lett. **18**(19), 1654–1656 (1993).
20. J. Collins, "Change in the infra-red absorption spectrum of water with temperature," Phys. Rev. **26**(6), 771–779 (1925).

1. Introduction

Optical parametric oscillators (OPOs) are capable of generating femtosecond pulses that are tunable over broad spectral ranges in the ultraviolet, visible, near-infrared (NIR), and mid-infrared wavelengths [1–4]. These devices are attractive for such applications as ultrafast time-resolved spectroscopy and nonlinear optical microscopy [5,6]. Recently, efficient terahertz (THz) generation in an NIR OPO via the intracavity difference-frequency mixing of two resonating optical waves in quasi-phase matched (QPM) GaAs has been reported [7]. In addition, dual-comb Fourier transform spectroscopy using two nonlinear crystals in a singly resonant OPO has been demonstrated [8].

In bulk nonlinear crystals, birefringent phase matching is generally used for efficient frequency conversion, which limits the choice of nonlinear crystals and the available wavelength regions. However, this limit has been significantly relaxed by the development of the periodic poling technique, in which the QPM can be additionally manipulated by adjusting the poling period. Nowadays, the periodic poling method is widely employed to a variety of crystals and for different nonlinear applications [9–12].

The mode-locked Ti:sapphire laser is the most common pumping source for femtosecond OPOs operating in the visible and NIR regions. Two different methods can be applied in order to obtain visible pulses from lower-energy 800-nm pulses generated by a Ti:sapphire laser. One is to double the pump energy through second-harmonic generation (SHG), such that visible pulses are generated via parametric down-conversion (PDC) [2]. The other method is to implement an SHG apparatus within an OPO cavity, which converts NIR pulses to visible pulses [13]. Although both schemes are relatively well established, the former method cannot produce NIR pulses, and the cavity design of the latter is somewhat complicated. As an advanced approach, the use of PPLN crystals possessing two grating designs in series were invented for the purpose of the intra-cavity SHG or SFG, where one is optimized for the OPO operation in the near-infrared while the other grating converts the signal or idler photons into visible ones [14,15].

In this paper, we report on the generation of visible femtosecond pulses through the SHG of signal photons or the sum-frequency generation (SFG) of signal and pump photon, which occurs at the gain material of an OPO operating in the NIR wavelength. The OPO in this study is based on magnesium-oxide-doped periodically poled lithium niobate (MgO:PPLN), and is synchronously pumped by femtosecond pulses from a Ti:sapphire laser. As compared to the conventional intra-cavity SHG method requiring additional SHG crystal and folding mirrors, the cavity configuration under this study is much simpler and the alignment is less difficult. It was found that high-order grating momentum of the PPLN crystal can enable efficient SHG or SFG process while the phase mismatch of the PDC is compensated by the

#247576 Received 7 Aug 2015; revised 12 Sep 2015; accepted 14 Sep 2015; published 21 Sep 2015

first-order grating momentum. Our system is unique in that a single PPLN grating plays dual roles.

2. Experimental results and discussion

A nonlinear MgO:PPLN crystal was doped with 5 mol% MgO in order to reduce the photorefractive effect and enable room temperature operation without heating [16]. The crystal has a length of 1-mm along the beam propagation and contains multiple gratings with the grating period (Λ) varying from 20.0 to 21.5 μm in 0.3 μm steps. Each grating had dimensions of 0.5 mm × 1 mm with a 0.2 mm separating gap. Note that, in most of the tests conducted in this study, the 21.2 μm grating period exhibited superior performance over the other periods. To reduce reflection losses, both sides of the crystal were anti-reflection-coated at the pump (780–830 nm) and signal (1000–1600 nm) wavelengths. The gain crystal was synchronously pumped using 87.6 MHz pulse trains from a Ti:Sapphire laser with 807 nm center wavelength and 100 fs pulse duration. A spherical mirror with a focal length of 100 mm (M8 in Fig. 1) focuses the pump beam into the crystal. We adopt a ring-cavity configuration, which prevents the losses in the linear-type cavity occurring when the signal propagates the crystal in opposite direction to the pump.

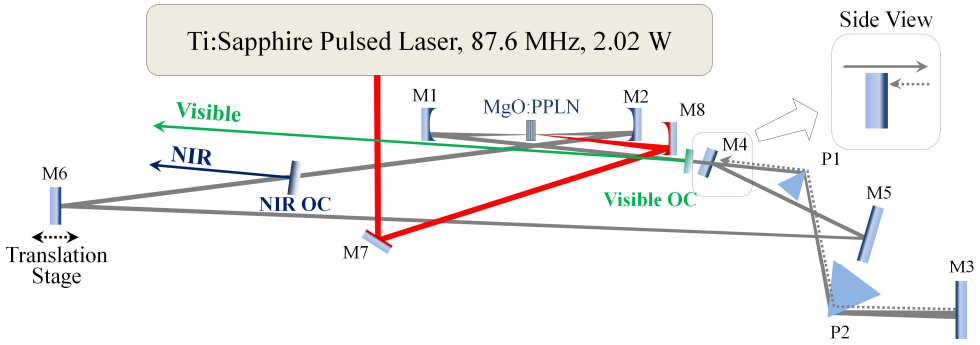

Fig. 1. Schematic diagram of synchronously-pumped optical parametric oscillator. MgO:PPLN: periodically poled magnesium-oxide-doped lithium niobate crystal; M1, M2: concave mirrors with radius of curvature (R) = 150 mm; M3–M7: flat mirrors, M8: concave mirror with R = 200 mm for pump-beam focusing; P1, P2: SF10 prisms; NIR OC: BK7 window with single-side anti-reflection coating at 1.0–1.6 μm for signal-pulse output coupling; Visible OC: long-pass filter with 900 nm cutoff for visible pulse output coupling.

A schematic diagram of the cavity is depicted in Fig. 1. M1 and M2 are concave mirrors with radius of curvature (R) of 150 mm, which folds the gain crystal. M3–M7 are flat mirrors. M8 is a concave mirror with an R of 200 nm. The dielectric coating of the cavity mirrors is designed to have high reflectivity of R > 99.8% and small negative group velocity dispersion (GVD) at $1060 < \lambda_{signal} < 1600$ nm. A prism pair (P1, P2) made of SF10 is used to control the GVD. The beam incident on M3 is leveled off slightly such that it is redirected at M4 toward M5. A plane BK7 window with anti-reflection coating on one side functions as a broadband output coupler (NIR OC in the figure), in which the out-coupling ratio can be adjusted by changing the incident angle [17]. In this study, out-coupling was set to 3% for the signal beam. To realize output coupling of the visible pulses without hampering the signal oscillation, we inserted a long-pass filter (Visible OC in the figure) with the cutoff at 900 nm, which is transparent in the NIR but reflects visible photons. For the pump beam, the focused diameter at the crystal was estimated to be about 110 μm with the divergence angle being less than 1°.

Due to the GVDs resulting from the PPLN crystal and the prism pair, the optical path length varies with the signal wavelength, and the gain is acting temporarily when the pump pulse sweeps within the 1-mm-thick crystal. Because of the GVD and the gain switching, the

#247576 Received 7 Aug 2015; revised 12 Sep 2015; accepted 14 Sep 2015; published 21 Sep 2015

signal wavelength building inside the cavity is determined such that the signal repetition is synchronized to the pump pulse trains. If the physical length of the cavity is adjusted by translating M6 mirror in Fig. 1, the synchronization condition changes and it leads to the tuning of the signal wavelength. Because the refractive index of PPLN depends on the temperature, the wavelength tuning in femtosecond OPO can also be fulfilled by changing the crystal temperature [18]. But, the refractive index change is rather small that the temperature increase by 100 °C in 1 mm thick PPLN crystal has an equivalent effect with the cavity adjustment by about 6 μm.

We examined the signal output variation under different GVD conditions, which was controlled by adjusting the prism pair. Figure 2 compares the spectra and field autocorrelations obtained under different GVD conditions for signal pulses near 1250 nm. The GVD polarity can be estimated from the slope of λ_{signal} versus the mirror displacement curves shown in the insets, which indicate that the signal tuning becomes less sensitive to the mirror displacement when the GVD is of large amount. The shortest pulse duration was obtained for the near-transform limited case, but the output was rather sensitive to mechanical fluctuations which can raise the stability issue. For the positive GVD, a jagged spectrum was obtained and ringing features were observed in the time-domain field profile. For the negative GVD, smooth Gaussian-like spectrum and single-robed autocorrelation without ringing were produced. To take use of the reliable tunability and good stability, we configured the OPO cavity at the negative GVD condition in the following studies. Note that higher stability under negative GVD has also been reported for mode-locked Ti:sapphire lasers [19].

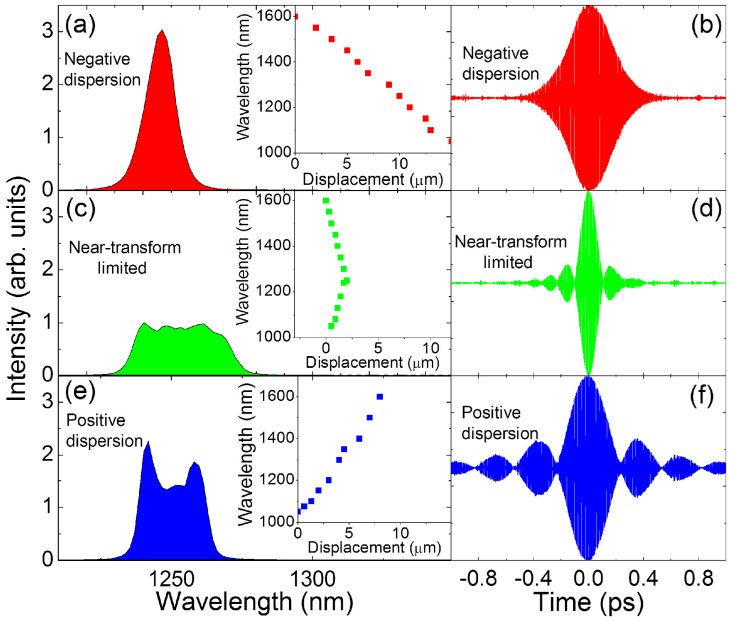

Fig. 2. (a,c,e) Spectrum and (b,d,f) field autocorrelation trace of signal pulses under different GVD conditions for signal pulses with the center wavelength near 1250 nm. The insets show the shift of the signal wavelength according to the M6 mirror displacement.

Figure 3 shows the signal pulse tunability, which was obtained by translating the M6 mirror with the other components fixed. With 12-μm displacement of M6, the signal pulse wavelength has continuously swept from 1050 to 1600 nm. The idler pulse (λ_{idler}), which is calculated from the relation $1/\lambda_{pump} = 1/\lambda_{signal} + 1/\lambda_{idler}$, covers the 1618–3487-nm wavelength range. The average powers plotted in the inset indicate that the signal is strong in the vicinity of λ_{signal} = 1100 nm for Λ = 21.2 μm. For the signal output at 1100 nm, a threshold pump

#247576 Received 7 Aug 2015; revised 12 Sep 2015; accepted 14 Sep 2015; published 21 Sep 2015

power of 530 mW was obtained with a slope efficiency of 29.8%, which yielded a conversion efficiency of 43.8% at the maximum pump power. The power decline observed at approximately 1400 nm is somehow attributed to the propagation loss in air caused by the water (H_2O) absorption [20]. The amount of the phase mismatch for the PDC (Δk_{PDC}) is also plotted in the inset of Fig. 3, which was calculated from Eq. (1) with n being the refractive index.

$$\Delta k_{\mathrm{PDC}} = \frac{2\pi \bullet n_{pump}}{\lambda_{pump}} - \frac{2\pi \bullet n_{signal}}{\lambda_{signal}} - \frac{2\pi \bullet n_{idler}}{\lambda_{idler}} - \frac{2\pi}{\Lambda} \tag{1}$$

Since the PDC at the PPLN crystal relies on the QPM mechanism for the compensation of the phase mismatch, the residual phase mismatch varies with the tuning of the signal wavelength. Then, the conversion efficiency from pump to signal photon will be influenced by the signal tuning. But, in spite of this phase mismatch the OPO has successfully operated over the full wavelength range (1050-1600 nm), which is defined by the high reflectivity of cavity mirrors.

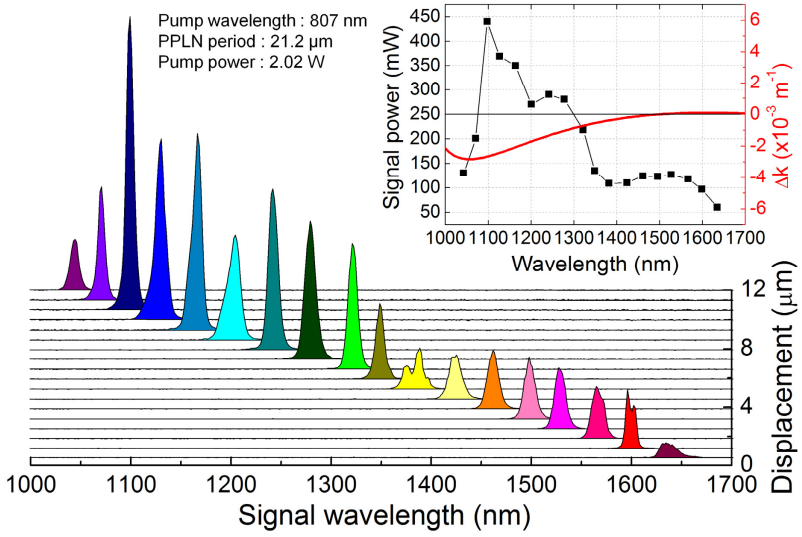

Fig. 3. Signal-pulse tunability obtained by adjusting cavity mirror M6 displacement while keeping other components fixed. Inset is the average signal power as a function of peak wavelength, together with the calculated phase mismatch (Δk) for the parametric down conversion.

Lithium niobate ($LiNbO_3$) crystals, having large nonlinear coefficients, are widely applied in nonlinear optical processes such as SHG, SFG, and difference frequency generation. With the out-coupling ratio of 3% in the proposed OPO system, the signal-pulse oscillating inside the OPO cavity has 33-fold greater intensity than the output signal, being comparable to or stronger than the pump pulse. If the crystal is infinitesimally thin, the SHG of signal pulses at the wavelength $\lambda_{SHG} = \lambda_{signal}/2$ or the SFG of the pump and signal photons, with $1/\lambda_{SFG} = 1/\lambda_{signal} + 1/\lambda_{pump}$, will be as efficient as the PDC process. However, Δk plays a decisive role when a crystal is as thick as 1 mm and other nonlinear processes can generally be neglected.

In this study, rather unexpectedly, strong visible pulses were generated through the SHG or SFG process within the PPLN crystal itself. The long-pass filter in Fig. 1, which is transparent at λ_{signal}, picks visible pulses out of the cavity. Figures 4(a) and 4(b), respectively, show the spectrum and temporal autocorrelation of the femtosecond pulses near 635 nm, which were generated from the SHG of the signal pulse at 1270 nm, with the energy being double to the signal photon. The spectrum exhibits jagged features, which hint at a strong Δk

#247576 Received 7 Aug 2015; revised 12 Sep 2015; accepted 14 Sep 2015; published 21 Sep 2015

gradient with respect to the wavelength. The temporal profile shows beating behavior with the full width at half maximum duration of approximately 500 fs. While the signal scales linearly with the pump power, the SHG power in Fig. 4(c) is quadratic to the pump power, being consistent with the SHG efficiency. On the other hand, the spectral and temporal feature are displaced in Figs. 4(d) and 4(e), for the visible pulses near 525 nm, which were generated from the SFG between the signal and pump photons. The energy is identical to the sum of a signal and a pump photon, and the temporal profile indicates that the pulse duration is approximately 400 fs. The output power of the SFG pulse is also super-linear to the pump power.

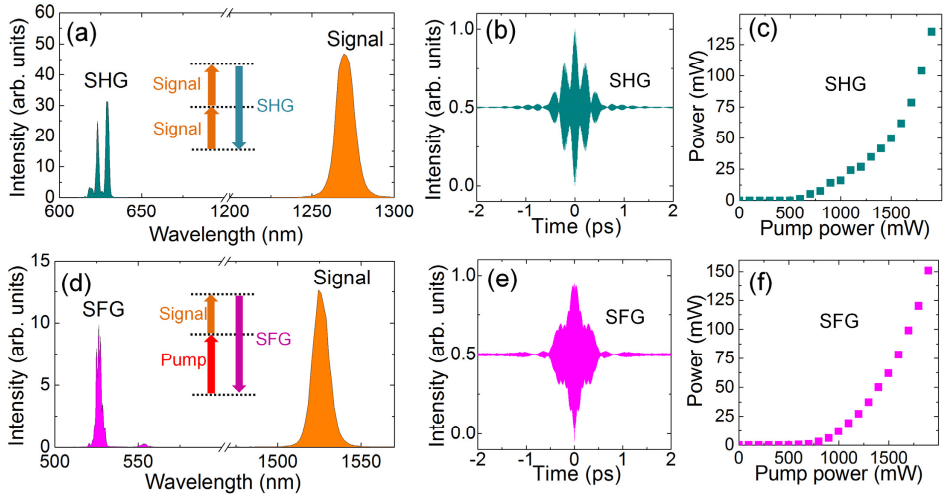

Fig. 4. (a,d) Spectrum and (b,e) temporal profile of the field autocorrelation, and (c, f) average powers as functions of pumping power, for the visible pulses created by the SHG or SFG process.

As the signal is tuned with the translation of M6, the visible pulses generated by the SHG or SFG will shift accordingly. Figure 5 shows the evolution of the visible pulse with the M6 displacement. Femtosecond pulses in the 455–540-nm wavelength range were obtained through the SFG process, while those from the SHG process span the 522–800-nm wavelength range. The beam profile of the beam at 542 nm generated via the SHG process, shown in the inset of Fig. 5, demonstrates the TEM_{00} spatial mode. As regard to the stability, for the case of λ_{SHG} = 542 nm, the peak-to-peak fluctuation over a duration of 2 hours was measured to be less than 3.5%.

#247576 Received 7 Aug 2015; revised 12 Sep 2015; accepted 14 Sep 2015; published 21 Sep 2015

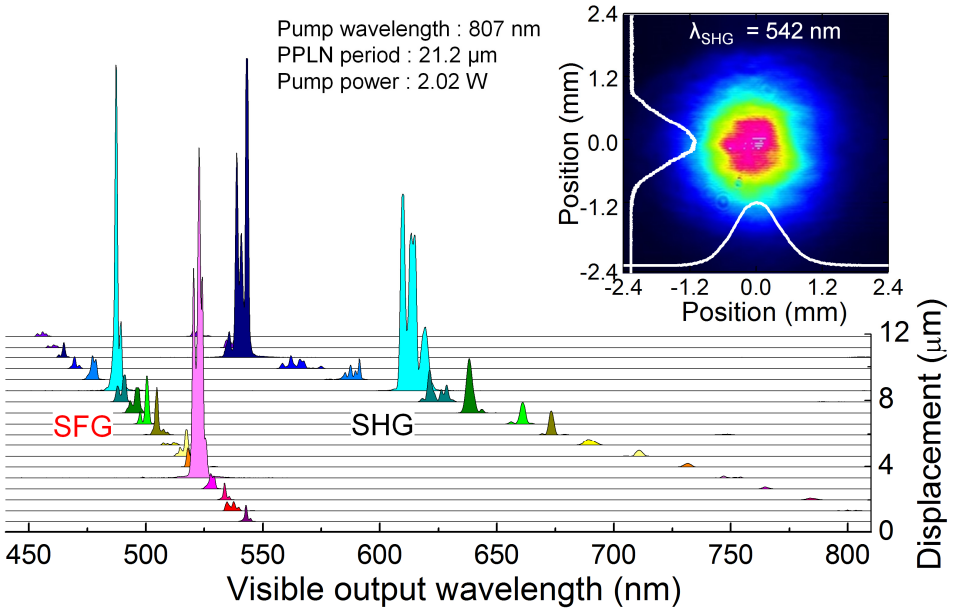

Fig. 5. Tunability of visible femtosecond pulses generated via the SFG and SHG processes, achieved through the adjustment of cavity mirror M6. Inset is the beam profile of visible pulses at 542 nm generated from the SHG process.

In Fig. 6(a), the average powers of the visible pulses are plotted as functions of the peak wavelength. While the signal is continuously tuned over the broad wavelength region, the SHG or SFG process generates reasonably high power only at specific wavelengths. The power is over 80 mW at λ_{SFG} = 483 nm and 522 nm for the case of SFG and at λ_{SHG} = 534 nm and 612 nm for the SHG process, but it is relatively low at other wavelengths. Those wavelengths generating bright visible pulses has shifted by 10~15 nm as the grating period was changed from 20.0 to 21.5 μm.

The output of visible pulses must be dependent on the efficiency of the SHG or SFG process. Since periodically poled structure can provide higher-order grating wavevectors (2, 3, or 4k_G), we have incorporated those in calculating the phase mismatch Δk of the nonlinear processes. As Fig. 6(b) reveals, the QPM of the SFG process is satisfied at λ_{SFG} = 483 nm and λ_{SFG} = 522 nm with the inclusion of 4th- and 3rd-order grating momentum, respectively. And the QPM for the SHG process locates at λ_{SHG} = 534 nm and λ_{SHG} = 612 nm with the 3rd- and 2nd-order grating momentum, respectively. For both nonlinear processes, the QPM wavelengths of high-orders well coincide with the positions of bright visible pulses in Fig. 6(a). This indicates that even when the grating design of first-order was optimized for the PDC process, higher-order QPM can provide efficient SFG or SHG process. In contrast to the smooth tuning of the signal pulse in Fig. 3, the intra-cavity SHG or SFG in Fig. 6 is found to be much sensitive to the phase mismatch of high-order QPMs. Taking it into account that the tunability of the PDC process for generating near-infrared photons is good even with a single grating period, if it is integrated with the fan-out type grating structure to provide efficient SHG or SFG at broader wavelengths, the tuning capability of this system will be improved considerably. Producing visible femtosecond pulses together with signal and idler pulses, the OPO system can be advantageous in studying ultrafast phenomena of various materials.

#247576 Received 7 Aug 2015; revised 12 Sep 2015; accepted 14 Sep 2015; published 21 Sep 2015

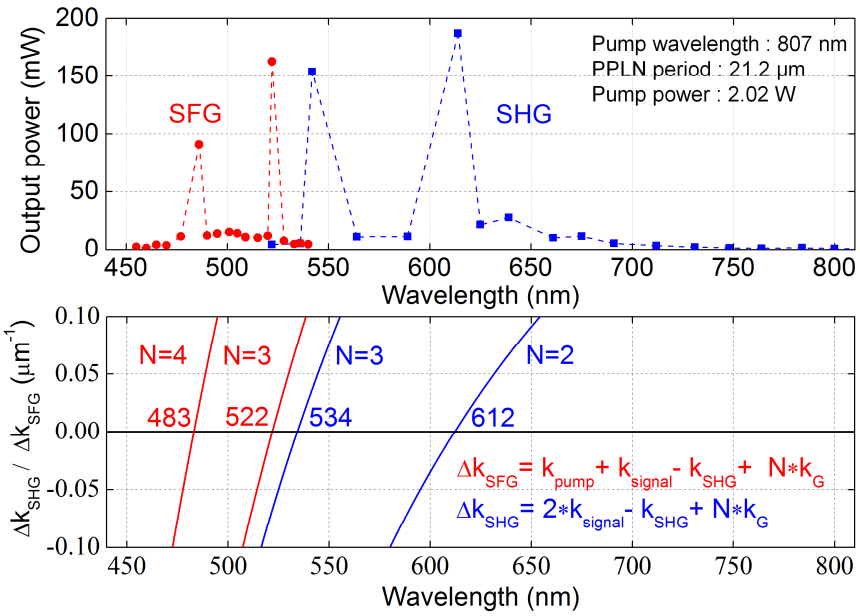

Fig. 6. (a) Average output powers of visible pulses generated through the SFG or SHG process as functions of the peak wavelength. (b) Phase mismatches (Δk) calculated with including 2nd- and 3rd- order grating wavevectors for SHG process and the 3rd- and 4th-order grating wavevectors for SFG process.

3. Conclusion

In an OPO operating in the near-infrared wavelength, we demonstrated on the generation of visible femtosecond pulses through the PDC and the intra-cavity SHG or SFG at the same PPLN crystal. When the cavity length was changed, the signal wavelength was continuously tuned in the 1050–1600-nm range with the grating period of Λ = 21.2 μm. Simultaneously with the near-infrared femtosecond pulses, visible pulses in the range of 522–800 and 455–540 nm were generated through the intra-cavity SHG of signal photons and through the SFG of the pump and signal photons, respectively. For the specific wavelengths such as λ_{SFG} = 483 and 522 nm for the SFG and λ_{SHG} = 534 and 612 nm for SHG, at which the QPM condition could be satisfied with the inclusion high-order grating wavevectors, the output power over 80 mW was obtained with the conversion efficiency reaching up to 9.2%. As it is widely tunable in the near-infrared and visible region, the OPO system in this study will be useful in such applications as time-resolved spectroscopy and multiphoton microscopy.

Acknowledgments

This work was supported by the National Research Foundation of Korea (NRF) grant funded by the Korean government (2013R1A2A2A01067707). GHK acknowledges the financial support from the project named Development of optical instruments for the creative industries (D34500) by Korea Basic Science Institute.

#247576 Received 7 Aug 2015; revised 12 Sep 2015; accepted 14 Sep 2015; published 21 Sep 2015